The Z+photon and diphoton decays of the Higgs boson as a joint probe of low energy SUSY models

Junjie Cao[1,2], Lei Wu[3], Peiwen Wu[3], Jin Min Yang[3]

[1] *Department of Physics, Henan Normal University, Xinxiang 453007, China*

[2] *Center for High Energy Physics, Peking University, Beijing 100871, China*

[3] *State Key Laboratory of Theoretical Physics,*

Institute of Theoretical Physics, Academia Sinica, Beijing 100190, China

Abstract

In light of recent remarkable progress in Higgs search at the LHC, we study the rare decay process $h \to Z\gamma$ and show its correlation with the decay $h \to \gamma\gamma$ in low energy SUSY models such as CMSSM, MSSM, NMSSM and nMSSM. Under various experimental constraints, we scan the parameter space of each model, and present in the allowed parameter space the SUSY predictions on the $Z\gamma$ and $\gamma\gamma$ signal rates in the Higgs production at the LHC and future e^+e^- linear colliders. We have following observations: (i) Compared with the SM prediction, the $Z\gamma$ and $\gamma\gamma$ signal rates in the CMSSM are both slightly suppressed; (ii) In the MSSM, both the $Z\gamma$ and $\gamma\gamma$ rates can be either enhanced or suppressed, and in optimal case, the enhancement factors can reach 1.2 and 2 respectively; (iii) In the NMSSM, the $Z\gamma$ and $\gamma\gamma$ signal rates normalized by their SM predictions are strongly correlated, and vary from 0.2 to 2; (iv) In the nMSSM, the $Z\gamma$ and $\gamma\gamma$ rates are greatly reduced. Since the correlation behavior between the $Z\gamma$ signal and the $\gamma\gamma$ signal is so model-dependent, it may be used to distinguish the models in future experiments.

PACS numbers: 14.80.Da,14.80.Ly,12.60.Jv

I. INTRODUCTION

Based on the measurements of $\gamma\gamma$ and ZZ^* channels the ATLAS and CMS collaborations have independently provided compelling evidence for a bosonic resonance around 125-126 GeV [1]. This is a great triumph for particle physics, but it also leads to a host of new questions about the nature of the boson. So far there exist large uncertainties in determining the rates of the two channels, and meanwhile, observation of the boson through other signals, such as $b\bar{b}$ and $\tau^+\tau^-$ channels, is still far away from becoming significant[2]. So although the preliminary data of the LHC indicate that the boson closely resembles the Higgs boson in the Standard Model (SM), the deficiencies of the SM itself such as gauge hierarchy problem suggest new physics explanation of the boson. Obviously, in order to decide the right underlying theory, the LHC should exhaust its potential to measure the decay channels of the boson as accurately as possible in its high luminosity phase.

Among the decay modes of the Higgs-like boson h, the diphoton channel plays a very important role in determining its mass, spin and parity[3]. At the same time, since the diphoton channel is mediated by loops of charged particles, it also acts as a sensitive probe to new physics. In fact, this feature has been widely utilized to explain the excess of the diphoton signal over its SM Higgs boson hypothesis reported by the ATLAS and CMS collaborations [4–14]. In this note, we concentrate on another decay mode $h \to Z\gamma$. In the SM, the branching ratio of this decay is about two thirds of that for the diphoton decay, and just like the diphoton signal, it can provide a clean final-state topology in determining the properties of the boson, such as its mass, spin and parity[15]. Moreover, since new charged particles affecting the diphoton decay can also contribute to the $Z\gamma$ decay, the two decay modes should be correlated, and therefore studying them in a joint way can reveal more details about the underlying physics. Albeit the advantages, in contrast to the diphoton decay which has been intensively studied, the $Z\gamma$ decay was paid little attention in the past. For example, so far only a few works have been devoted to this decay in new physics models [16, 17], and until very recently have the CMS and ATLAS collaboration set an upper limit on the ratio $\sigma_{Z\gamma}/\sigma^{\rm SM}_{Z\gamma} < 10$[18]. Here we remind that, although the $Z\gamma$ signal suffers from large irreducible background at the LHC[18], at the next generation linear colliders with given collision energy, the Higgs event from the process $e^+e^- \to Zh \to ZZ\gamma$ can be easily reconstructed, which is very helpful in suppressing the background for such signal. So there

is good prospect to measure accurately this decay in future.

In the following, we focus on the $Z\gamma$ decay channel of the SM-like Higgs boson h in low energy supersymmetric models such as the Constrained Mimimal Supersymmetric Standard Model (CMSSM), the Minimal Supersymmetric Standard Model (MSSM), the Next-to-Minimal Supersymmetric Standard Model (NMSSM) and the Nearly Minimal Supersymmetric Standard Model (nMSSM). We investigate the $Z\gamma$ signal of the Higgs production at the LHC and future e^+e^- linear colliders, and especially, we show its correlations with the $\gamma\gamma$ signal. As we will show below, the $Z\gamma$ signal rate may be either enhanced or suppressed in SUSY, and its correlation behavior is so model-dependent that it may be utilized to distinguish the models in high luminosity phase of the LHC.

This work is organized as follows. In Section II we introduce the basic features of the SUSY models and present some formulae relevant to our calculation. In Section III we first discuss the effects of new charged SUSY particles on the partial decay widths of $h \to Z\gamma$, then we study in a comparative way the $Z\gamma$ and $\gamma\gamma$ signal rates of the Higgs production at different colliders. Finally, we draw the conclusions in Section IV. Various couplings used in the calculation are given in the Appendix.

II. THE MODELS AND ANALYTIC FORMULAE

In a low energy supersymmetric gauge theory, the explicit form of its Lagrangian is determined by the gauge symmetry, superpotential and also soft breaking terms. As for the four models considered in this work, their differences mainly come from the superpotential, which is the source for the Yukawa interactions of fermions and self interactions of scalars.

MSSM and CMSSM : The MSSM and CMSSM contain two Higgs doublets H_u, H_d and so they predict five physical Higgs bosons, of which two are CP-even, one is CP-odd and two are charged. Their superpotential is given by

$$W^{\rm MSSM} \;=\; W_F + \mu \hat{H}_u \cdot \hat{H}_d, \tag{1}$$

where W_F denotes the Yukawa interaction, and it takes following from

$$W_F \;=\; \overline{\hat{u}} Y_u \hat{Q} \cdot \hat{H}_u - \overline{\hat{d}} Y_d \hat{Q} \cdot \hat{H}_d - \overline{\hat{e}} Y_e \hat{L} \cdot \hat{H}_d. \tag{2}$$

After considering appropriate soft breaking terms, one can write down the Higgs potential

as

$$
\begin{aligned}
V^{MSSM} &= (|\mu|^2 + m_{H_u}^2)|H_u^0|^2 + (|\mu|^2 + m_{H_d}^2)|H_d^0|^2 \\
&- (B\mu H_u^0 H_d^0 + \text{h.c.}) + \frac{1}{8}(g_2^2 + g_1^2)(|H_u^0|^2 - |H_d^0|^2)^2,
\end{aligned} \tag{3}
$$

where m_{H_u}, m_{H_d} and B are soft parameters with mass dimension, terms proportional to $|\mu|^2$ come from the superpotential (so called F-term), and the last term comes from gauge symmetry (called D-term). This potential indicates that, after the electroweak symmetry breaking, the μ-parameter is related to the Higgs vacuum expectation value (vev) and so its value should be around the electroweak scale. But on the other hand, since μ as the only parameter with mass dimension appears in the superpotential, it should naturally lie at the SUSY breaking scale. Such a tremendously large scale gap is usually referred as the μ-problem [19].

Different from the general MSSM where all soft breaking parameters are independent[20], the CMSSM [22] assumes following universal soft breaking parameters at SUSY breaking scale (usually chosen at the Great Unification scale)

$$
M_{1/2}\ ,\ M_0\ ,\ A_0\ , \tan\beta\ ,\ \text{sign}(\mu), \tag{4}
$$

with $M_{1/2}$, M_0 and A_0 denoting gaugino mass, scalar mass and trilinear interaction coefficient respectively, and evolves the four parameters down to weak scale to get all the soft breaking parameters of the low energy MSSM. In this sense, the parameter space of the CMSSM should be considered as a subset of that for the MSSM, and so is its phenomenology.

NMSSM and nMSSM : In order to solve the μ-problem in the MSSM, various singlet extensions of the MSSM were proposed in history, and among them the most well known models include the NMSSM and nMSSM. The superpotentials of these two models are respectively given by [23, 24]

$$
W^{\text{NMSSM}} = W_F + \lambda \hat{S}\hat{H}_u \cdot \hat{H}_d + \frac{\kappa}{3}\hat{S}^3, \tag{5}
$$

$$
W^{\text{nMSSM}} = W_F + \lambda \hat{S}\hat{H}_u \cdot \hat{H}_d + \xi_F M_{\text{n}}^2 \hat{S}, \tag{6}
$$

where λ, κ and ξ_F are dimensionless parameters of order 1, and the dimensionful parameter M_n may be naturally fixed at weak scale in certain basic framework where the parameter is generated at a high loop level[24]. One attractive feature of the both models comes from the fact that, after the real scalar component of $\hat{S}$ develops a vev $\langle S \rangle$, an effective μ parameter

of $\mathcal{O}(100\text{GeV})$ is naturally generated by $\mu_{eff} = \lambda\langle S\rangle$. Another attractive feature is due to the Higgs self interactions, the squared mass of the SM-like Higgs boson gets an additional contribution $\lambda^2 v^2 \sin^2 2\beta$, and furthermore, it can also be enhanced by the doublet-singlet mixing[12]. This feature is very useful to alleviate the fine tuning of the models[12].

Noting that the tadpole term in the nMSSM only affects the masses of the Higgs bosons, one can easily conclude that the interactions in the nMSSM are identical to those in the NMSSM with $\kappa = 0$. This fact enables us to modify the package NMSSMTools to study the phenomenology of the nMSSM[25]. As analyzed in [25], in the nMSSM the lightest neutralino as the dark matter candidate is light and singlino dominated, and it must annihilate through exchanging a resonant light CP-odd Higgs boson to get the correct relic density. As a result, the SM-like Higgs boson tends to decay dominantly into light neutralinos or other light Higgs boson so that its total width enlarges greatly. This character is rather peculiar and different from the predictions of the NMSSM[26].

Formula in calculation: In order to study the $h \to Z\gamma$ decay and its correlation with the $h \to \gamma\gamma$ decay in SUSY, we define following normalized rates at the LHC and the international linear collider (ILC) as

$$R_{Z\gamma} \equiv \frac{\sigma(pp \to h \to Z\gamma)}{\sigma_{\rm SM}(pp \to h \to Z\gamma)} = \frac{\sigma_{tot}}{\sigma_{tot}^{\rm SM}} \frac{{\rm Br}(h \to Z\gamma)}{{\rm Br}_{\rm SM}(h \to Z\gamma)} \simeq \left(\frac{C_{hgg}}{C_{hgg}^{\rm SM}}\right)^2 \cdot \frac{\Gamma_{Z\gamma}(h)}{\Gamma_{Z\gamma}^{SM}(h)} \cdot \frac{\Gamma_{tot}^{\rm SM}(h)}{\Gamma_{tot}(h)}, \quad (7)$$

$$R_{\gamma\gamma} \equiv \frac{\sigma(pp \to h \to \gamma\gamma)}{\sigma_{\rm SM}(pp \to h \to \gamma\gamma)} = \frac{\sigma_{tot}}{\sigma_{tot}^{\rm SM}} \frac{{\rm Br}(h \to \gamma\gamma)}{{\rm Br}_{\rm SM}(h \to \gamma\gamma)} \simeq \left(\frac{C_{hgg}}{C_{hgg}^{\rm SM}}\right)^2 \cdot \frac{\Gamma_{\gamma\gamma}(h)}{\Gamma_{\gamma\gamma}^{SM}(h)} \cdot \frac{\Gamma_{tot}^{\rm SM}(h)}{\Gamma_{tot}(h)}, \quad (8)$$

$$\mathcal{K}_{Z\gamma} \equiv \frac{\sigma(e^+e^- \to Zh \to ZZ\gamma)}{\sigma_{\rm SM}(e^+e^- \to Zh \to ZZ\gamma)} \simeq \left(\frac{C_{hZZ}}{C_{hZZ}^{\rm SM}}\right)^2 \cdot \frac{\Gamma_{Z\gamma}(h)}{\Gamma_{Z\gamma}^{SM}(h)} \cdot \frac{\Gamma_{tot}^{\rm SM}(h)}{\Gamma_{tot}(h)}, \quad (9)$$

$$\mathcal{K}_{b\bar{b}} \equiv \frac{\sigma(e^+e^- \to Zh \to Zb\bar{b})}{\sigma_{\rm SM}(e^+e^- \to Zh \to Zb\bar{b})} \simeq \left(\frac{C_{hZZ}}{C_{hZZ}^{\rm SM}}\right)^2 \cdot \frac{\Gamma_{b\bar{b}}(h)}{\Gamma_{b\bar{b}}^{SM}(h)} \cdot \frac{\Gamma_{tot}^{\rm SM}(h)}{\Gamma_{tot}(h)}. \quad (10)$$

Here C_{hgg} and C_{hZZ} are the couplings of the Higgs boson to gluons and Zs respectively, and $\Gamma_{Z\gamma}(h)$, $\Gamma_{\gamma\gamma}(h)$ and $\Gamma_{b\bar{b}}(h)$ are the widths for the decays $h \to Z\gamma$, $h \to \gamma\gamma$ and $h \to b\bar{b}$ respectively. In getting these formula, we neglect SUSY radiative correction to the signals. These corrections are expected to be at few percent level given that heavy sparticles are preferred by current LHC experiments.

In SUSY, the decays $h \to Z\gamma$ and $h \to \gamma\gamma$ get new contributions from the loops mediated by charged Higgs bosons, sfermions (including stops, sbottoms and staus) as well as

charginos, and consequently, the formula of $\Gamma_{Z\gamma}$ and $\Gamma_{\gamma\gamma}$ are modified by

$$\Gamma_{Z\gamma}(h) = \frac{G_F^2 m_W^2 \alpha\, m_h^3}{64\,\pi^4}\left(1-\frac{m_Z^2}{m_h^2}\right)^3 \left|\mathcal{A}_W^{Z\gamma}+\mathcal{A}_t^{Z\gamma}+\mathcal{A}_{\tilde{f}}^{Z\gamma}+\mathcal{A}_{H^\pm}^{Z\gamma}+\mathcal{A}_{\chi^\pm}^{Z\gamma}\right|^2, \tag{11}$$

$$\Gamma_{\gamma\gamma}(h) = \frac{G_F \alpha^2 m_h^3}{128\sqrt{2}\pi^3}\left|\mathcal{A}_W^{\gamma\gamma}+\mathcal{A}_t^{\gamma\gamma}+\mathcal{A}_{\tilde{f}}^{\gamma\gamma}+\mathcal{A}_{H^\pm}^{\gamma\gamma}+\mathcal{A}_{\chi^\pm}^{\gamma\gamma}\right|^2, \tag{12}$$

where $\mathcal{A}_i$ $(i = W, t, \tilde{f}, H^\pm, \chi^\pm)$ denote the contribution from particle i mediated loops, and their explicit expressions are listed in Appendix. Note that our expressions differ from those presented in [27] in two aspects. One is we have an overall minus sign for the new contributions $\mathcal{A}_{H^\pm}$, $\mathcal{A}_{\tilde{f}}$ and $\mathcal{A}_{\chi^\pm}$, and an additional factor 2 for the sfermion contributions. This sign difference was also observed recently in [21]. The other difference is we have included in a neat way the contributions from the loops with two particles (such as $\tilde{f}_1$ and $\tilde{f}_2$ or $\chi_1^\pm$ and $\chi_2^\pm$) running in them. Such contributions were considered to be negligibly small [27], but our results indicate that sometimes they may play a role. Also note that in the well-known SUSY package FeynHiggs [29], the decay $h \to Z\gamma$ is actually not calculated, and in the package NMSSMTools [28], the decay is calculated only by considering the contributions from the SM particles and the charged Higgs boson. We improve these packages by inserting our codes for $h \to Z\gamma$ into them.

III. NUMERICAL CALCULATION AND DISCUSSIONS

In our calculation, we first scan over the parameter spaces of the four models by imposing various experimental constraints, then for the surviving samples we investigate the features of the $h \to Z\gamma$ and $h \to \gamma\gamma$ decays. In performing the scans, we adopt the strategy described in [12], and we have following improvements

- Noting the decay rate $h \to Z\gamma$ is sensitive to the chiral mixing angle $\theta_{\tilde{\tau}}$ in the scalar τ sector (see below), we treat M_{L3} and M_{E3} as independent parameters and vary them in the ranges:

$$100\ \text{GeV} < M_{L3}, M_{E3} < 1\ \text{TeV}. \tag{13}$$

- We use the latest results of the XENON100 experiment in dark matter direct detection[30], the LHCb measurement of $B_s \to \mu^+\mu^-$ [31] and the CMS search for non-SM Higgs boson from the channel $H/A \to \tau^+\tau^-$[32] to limit the parameter spaces.

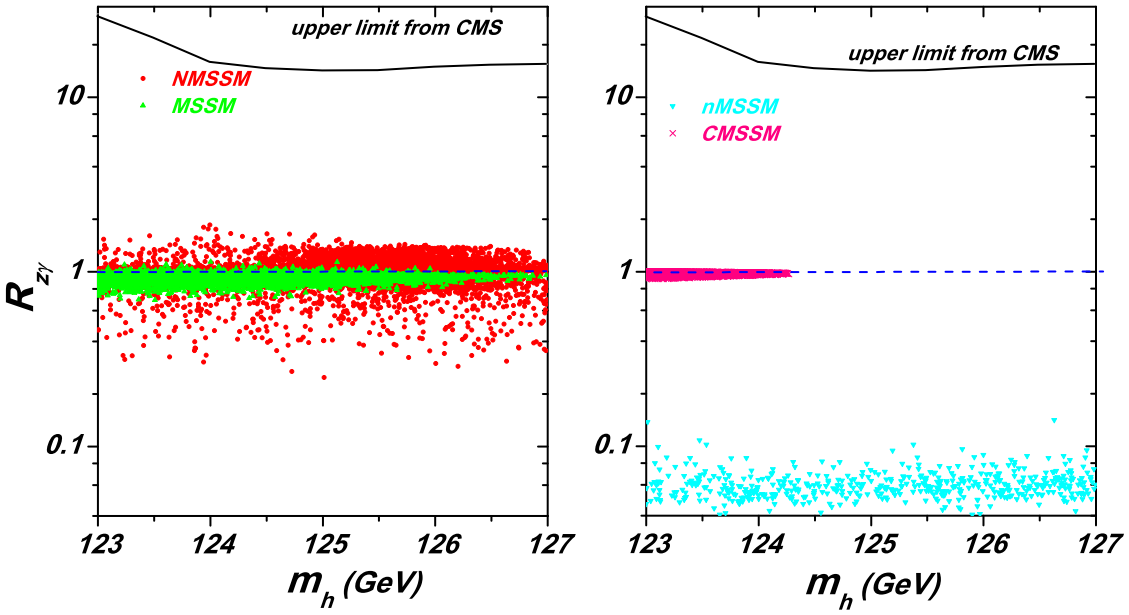

FIG. 1: The scatter plots of the surviving samples in the four models, projected on the $R_{Z\gamma} - m_h$ plane. Here $R_{Z\gamma} = \sigma(pp \to h \to Z\gamma)/\sigma_{\rm SM}(pp \to h \to Z\gamma)$ denotes the normalized $Z\gamma$ signal rate in the SM-like Higgs boson production at the LHC, and the black line represents its upper limit set by the CMS collaboration [18].

The samples obtained in this way predicting 123 GeV$< m_h <$ 127 GeV, are able to explain the muon magnetic moment anomaly at 2σ level and meanwhile satisfy various experimental constraints. Note for the NMSSM samples, we restrict λ to vary from 0.5 to 0.7. The property of the SM-like Higgs boson for these samples, as pointed out in [12], is quite different from that of the MSSM.

In Fig.1 we project the surviving samples on the plane of the $Z\gamma$ signal rate at the LHC versus the SM-like Higgs boson mass in the four SUSY models. We also show the CMS bound on the signal rate in the figure[18]. This figure indicates that compared with its SM prediction, the $Z\gamma$ signal rate in the MSSM and NMSSM may be either enhanced or suppressed, and in particular, the NMSSM can alter the rate by more than 50%. In contrast, the rate is always slightly suppressed in the CMSSM and severely suppressed in the nMSSM. We checked that, for the CMSSM the suppression is due to the increase of the partial width of $h \to b\bar{b}$ [11], while for the nMSSM, it is due to the open up of new decay channels $h \to \tilde{\chi}\tilde{\chi}, AA$, where $\tilde{\chi}$ and A denote light neutralino and CP-odd Higgs boson respectively[25]. This figure also indicates that the SM-like Higgs boson mass can not reach

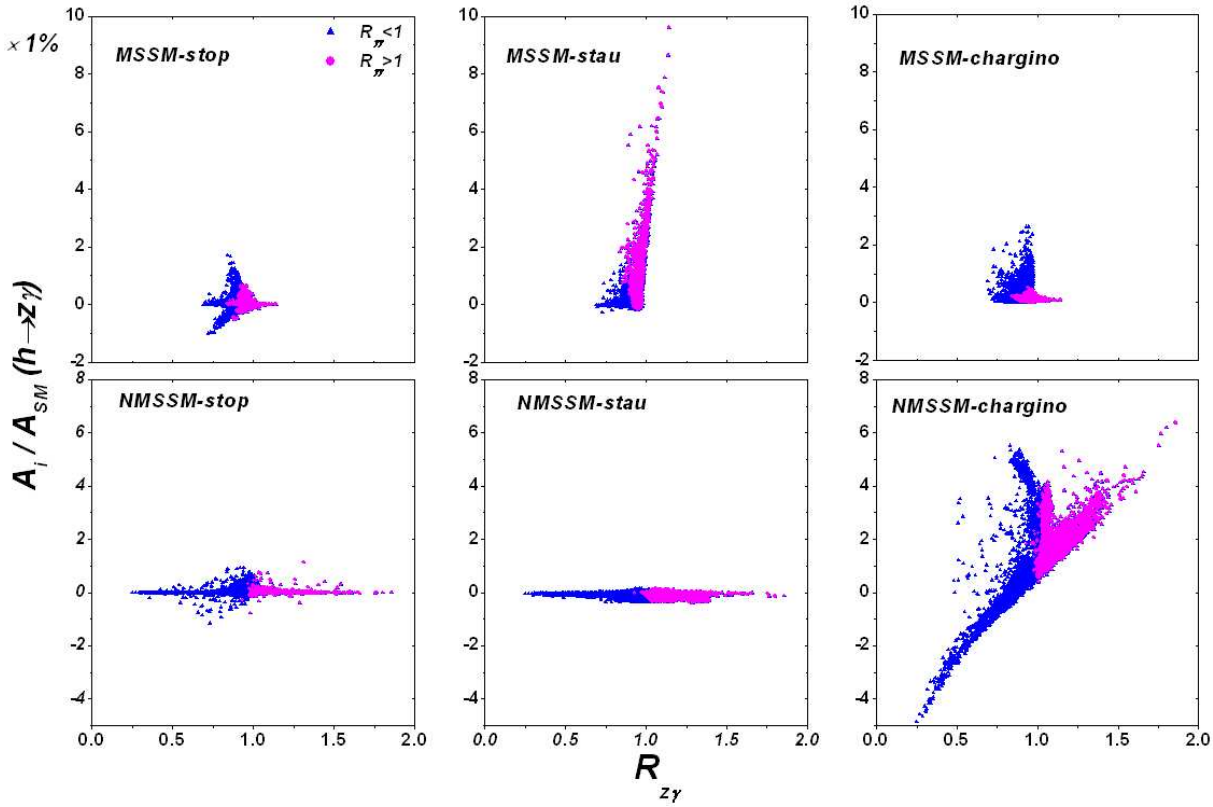

FIG. 2: Same as Fig.1, but showing the normalized sparticle contributions to the amplitude of $h \to Z\gamma$ in the MSSM and NMSSM. The magenta bullets and blue triangles represent the samples with $R_{\gamma\gamma} > 1$ and $R_{\gamma\gamma} < 1$ respectively.

the measured central value of 125 GeV in the CMSSM. The reason is that we have required the theory to explain the muon magnetic moment anomaly so that the parameters M_0 and $M_{1/2}$ are upper bounded[11].

Next we focus on the MSSM and NMSSM. In Fig.2 we exhibit the contributions of different sparticles to the amplitude of $h \to Z\gamma$ in the two models. Since the sbottoms and charged Higgs bosons have little effect on the amplitude, we do not show their contributions. This figure tells us following facts:

(1) In the MSSM, the potentially largest contribution comes from $\tilde{\tau}$ loops, which can alter the SM amplitude by about 10%. In contrast, the $\tilde{t}$ contribution is small, usually changing the amplitude by less than 3%. This feature can be well understood by the formula listed in Appendix. Explicitly speaking, in order to get a significant sfermion contribution, one necessary condition is $Y_{hLR} \sin 2\theta_{\tilde{f}}/m^2_{\tilde{f}_1}$ should be as large as possible, where Y_{hLR} denotes the chiral flipping coupling of higgs to sfermion, $\theta_{\tilde{f}}$ is the chiral

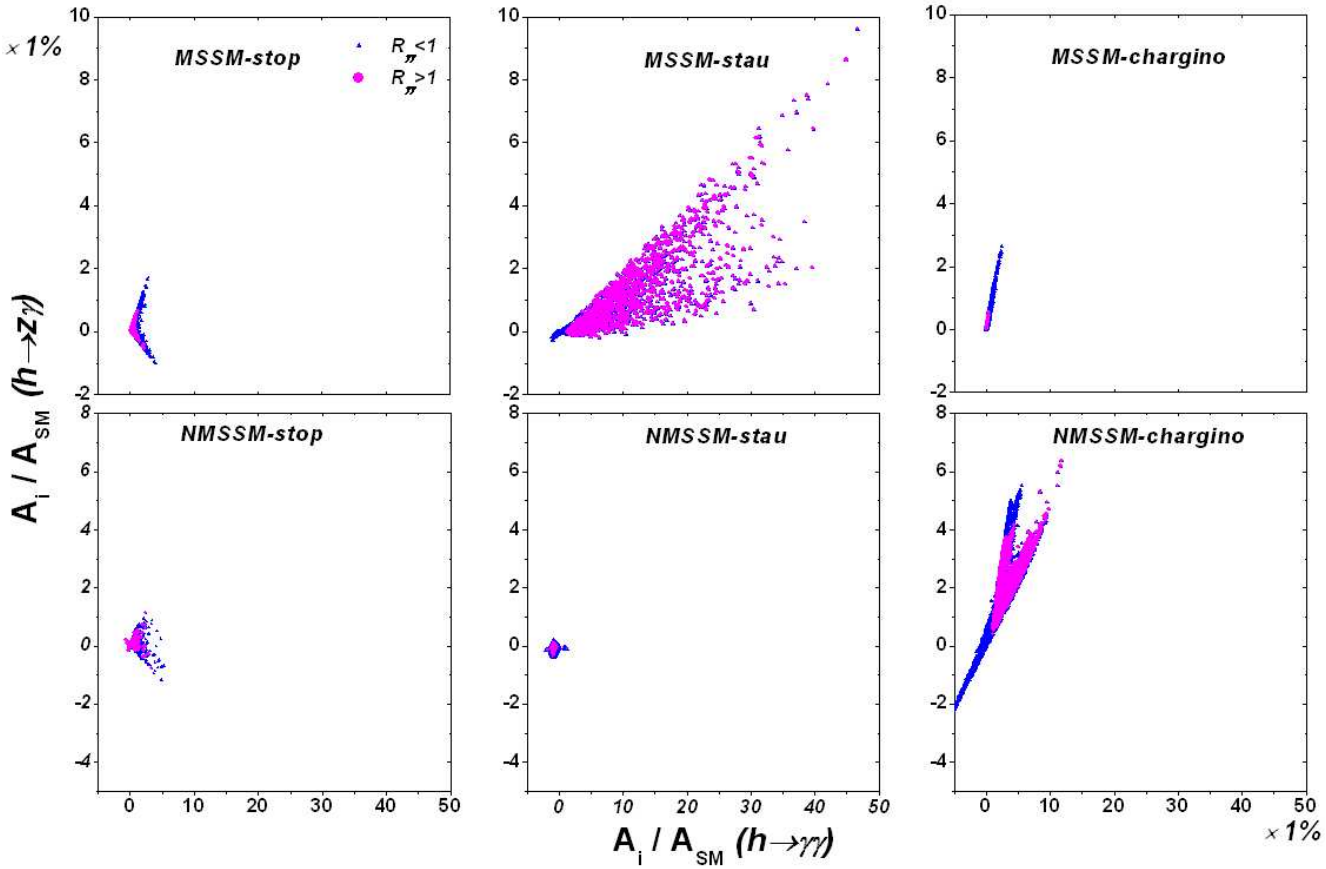

FIG. 3: Same as Fig.2, but showing the correlation of SUSY particle contribution to $h \to Z\gamma$ channel with that to $h \to \gamma\gamma$ channel.

mixing angle and $m_{\tilde{f}_1}$ denotes the lighter sfermion. As far as scalar top quark sector is concerned, a relatively light $\tilde{t}_1$ must accompany with a heavy $\tilde{t}_2$ in order to predict $m_h \simeq 125$GeV. Then even though A_t in this case may be very large, the chiral mixing angle $\theta_{\tilde{t}}$ is usually small, and consequently the $\tilde{t}$ contribution can never get significantly enhanced. While for the $\tilde{\tau}$ sector, both the parameters M_{L3} and M_{E3} are unlimited, and one can choose light $\tilde{\tau}$s and an appropriate $\theta_{\tilde{\tau}}$ to maximize the contribution. In this process, the value of $\mu \tan\beta$ and the splitting between M_{L3} and M_{E3} play an important role in determining the contribution size.

(2) In the MSSM, the chargino contribution is small and can only reach 3% and 0.5% for $R_{\gamma\gamma} < 1$ and $R_{\gamma\gamma} > 1$ cases respectively. The reason is in the MSSM, μ must be larger than 200GeV and 800GeV for the two cases, and consequently, the lighter chargino is gaugino-like and its coupling with h is small.

(3) In the NMSSM, the potentially largest contribution to the decay comes from chargino

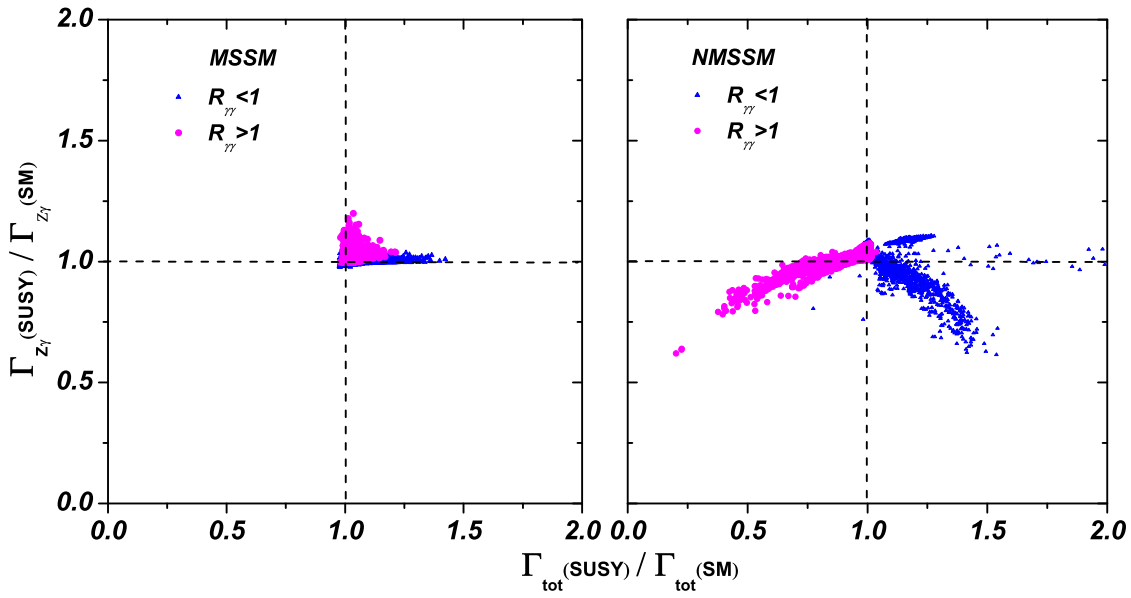

FIG. 4: Same as Fig.2, but projected on the plane of $\Gamma^{\rm SUSY}_{Z\gamma}/\Gamma^{\rm SM}_{Z\gamma}$ versus $\Gamma^{\rm SUSY}_{\rm total}/\Gamma^{\rm SM}_{\rm total}$.

loops with its size reaching 6% at most, while the magnitude of the $\tilde{\tau}$ contribution is always smaller than 1%. This is because in the NMSSM with large λ, μ is preferred to vary from 100GeV to 250GeV and $\tan\beta$ is usually less than 10[12]. As a result, the $h\bar{\tilde{\chi}}^{\pm}\tilde{\chi}^{\pm}$ coupling is enhanced by the sizable Higgsino component of $\tilde{\chi}^{\pm}$, while the $h\tilde{\tau}^*_L\tilde{\tau}_R$ coupling can not be pushed up by small $\mu\tan\beta$. Fig.2 also indicates that, due to the singlet component of h in the NMSSM, the $hb\bar{b}$ is suppressed and so is the partial width of $h\to b\bar{b}$. Consequently, $R_{Z\gamma}$ may be quite large even when the chargino contribution is small.

In Fig.3, we show the correlation of the amplitudes for $h\to Z\gamma$ and $h\to\gamma\gamma$. This figure indicates that in the two models, the $\tilde{t}$ contribution to the amplitude of $h\to Z\gamma$ correlates with that of $h\to\gamma\gamma$ by approximately linear relations, and even better in the chargino contribution. This is understandable since both the corrections come from the the same particles. This figure also indicates that the linear relation is spoiled for the $\tilde{\tau}$ contribution in the MSSM. We checked that this is because the θ_τ dependences of the two amplitudes are quite different, and meanwhile θ_τ in this work varies over a broad range. For example, if $M_{L3}\simeq M_{E3}$, we have $\theta_\tau\simeq\pi/4$. In this case, the $Z\tilde{\tau}^*_i\tilde{\tau}_i$ coupling and the $h\tilde{\tau}^*_1\tilde{\tau}_2$ coupling approach zero by accidental cancelation so that the $\tilde{\tau}$ contribution to $h\to Z\gamma$ is very small, while the contribution to $h\to\gamma\gamma$ is maximized since it is proportional to $\sin 2\theta_\tau$. On the

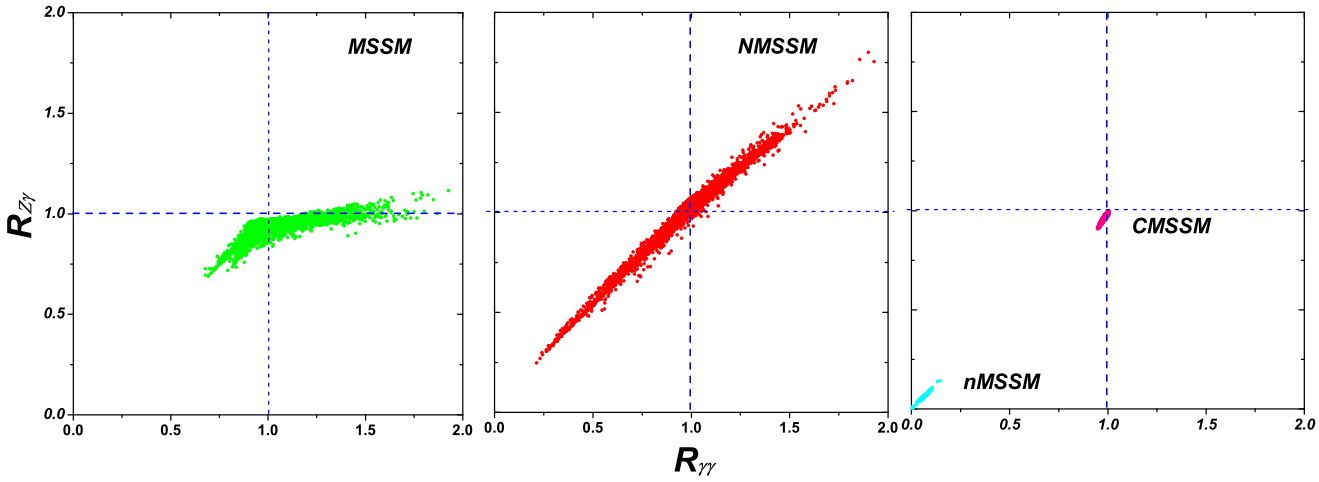

FIG. 5: Same as Fig.1, but showing the correlation between $R_{Z\gamma} = \sigma(pp \to h \to Z\gamma)/\sigma_{\rm SM}(pp \to h \to Z\gamma)$ and $R_{\gamma\gamma} = \sigma(pp \to h \to \gamma\gamma)/\sigma_{\rm SM}(pp \to h \to \gamma\gamma)$ in the four models.

other hand, if $|M_{L3}^2 - M_{E3}^2| \gg m_\tau \mu \tan\beta$, which means $\theta_\tau \to 0$, the contributions to $h \to Z\gamma$ and $h \to \gamma\gamma$ are all suppressed since their dominant contributions are proportional to $\sin 2\theta_\tau$.

Considering $R_{Z\gamma}$ is mainly determined by the partial width of $h \to Z\gamma$ and the total width of the SM-like Higgs boson, we present in Fig.4 the ratio of $\Gamma_{Z\gamma}^{\rm SUSY}/\Gamma_{Z\gamma}^{\rm SM}$ versus the ratio of $\Gamma_{\rm total}^{\rm SUSY}/\Gamma_{\rm total}^{\rm SM}$ for the two models. The left panel indicates that for almost all the samples in the MSSM the total and $Z\gamma$ partial width of the SM-like Higgs boson is larger than the corresponding SM predictions. These features originate from the enhanced decay width of $h \to b\bar{b}$ and the constructive contributions of the SUSY particles to the decay $h \to Z\gamma$ respectively. Interestingly, the largest increase of $\Gamma_{Z\gamma}$ occurs when $\Gamma_{tot} \simeq \Gamma_{tot}(SM)$. The right panel indicates that, in order to enhance the $Z\gamma$ signal in the NMSSM with large λ, the SM-like Higgs boson must have a small singlet component to suppress the partial width of $h \to b\bar{b}$. In this case, even though $\Gamma_{Z\gamma}$ is suppressed too, we have $\Gamma_{Z\gamma}/\Gamma_{Z\gamma}(SM) > \Gamma_{tot}/\Gamma_{tot}(SM)$. Moreover, as mentioned before, the $\Gamma_{Z\gamma}$ can be significantly enhanced by the chargino contribution.

Now let's summarize the $Z\gamma$ and $\gamma\gamma$ signal rates at the LHC in different SUSY models. This is shown in Fig.5. From this figure we have the following conclusions:

(a) In the MSSM, although the partial width of $h \to Z\gamma$ is enhanced by at most 20% (see Fig.4), due to the increase of the the Higgs width ad also due to the slight suppression of the hgg coupling [12], $R_{Z\gamma} > 1$ is achieved only for $R_{\gamma\gamma} \gtrsim 1.25$. The maximal

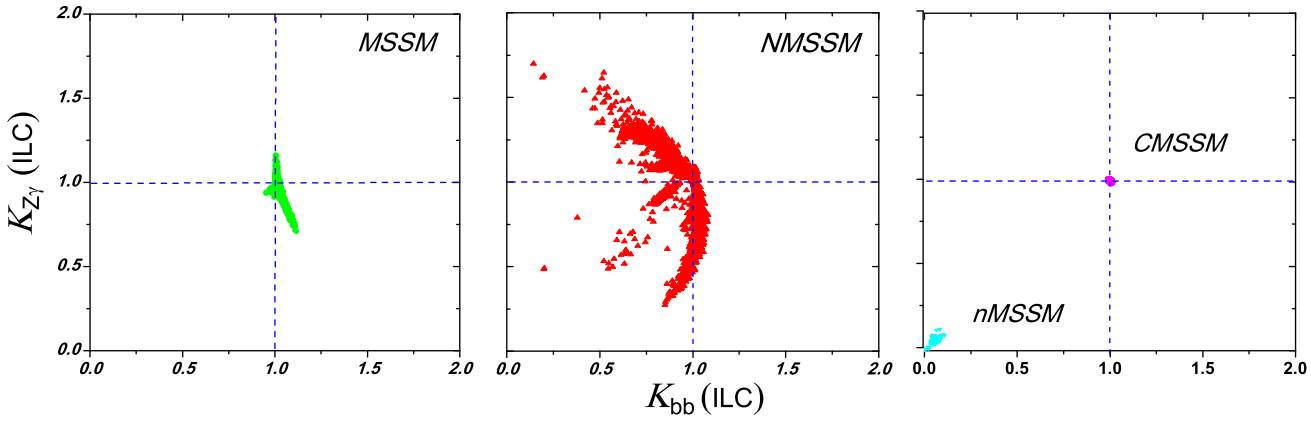

FIG. 6: Same as Fig.1, but showing the correlation between $\mathcal{K}_{Z\gamma} = \sigma(e^+e^- \to Zh \to ZZ\gamma)/\sigma_{\rm SM}(e^+e^- \to Zh \to ZZ\gamma)$ and $\mathcal{K}_{b\bar{b}} = \sigma(e^+e^- \to Zh \to Zb\bar{b})/\sigma_{\rm SM}(e^+e^- \to Zh \to Zb\bar{b})$ in the four models.

values of $R_{Z\gamma}$ and $R_{\gamma\gamma}$ are 1.2 and 2 respectively. Among the sparticle contributions to $R_{Z\gamma}$ and $R_{\gamma\gamma}$, the $\tilde{\tau}$ loops may play the dominant role. The difference for the two observables come from the fact that, for $\theta_\tau \simeq \pi/4$, the $\tilde{\tau}$ contribution to $R_{\gamma\gamma}$ is maximized, while that to $h \to Z\gamma$ approaches zero.

(b) In the NMSSM with large λ, the sparticle contributions to the amplitudes of $h \to Z\gamma$ and $h \to \gamma\gamma$ are at most 10%, and the main mechanism to alter the predictions of $R_{Z\gamma}$ and $R_{\gamma\gamma}$ is through tuning the $hb\bar{b}$ coupling by the singlet component of h. As a result, $R_{Z\gamma}$ and $R_{\gamma\gamma}$ are highly correlated, and both of them vary from 0.2 to 2.

(c) In the CMSSM and nMSSM, $R_{Z\gamma}$ and $R_{\gamma\gamma}$ are slightly and strongly suppressed respectively. As discussed before, in the CMSSM the suppression is due to the increase of the partial width for $h \to b\bar{b}$, while in the nMSSM, it is due to the open up of the exotic decay channels of h, i.e. $h \to \chi^0\chi^0, AA$.

Since the e^+e^- collider provides a clean environment to observe the decays $h \to Z\gamma$ and $h \to b\bar{b}$, we also investigate their normalized rates at the ILC. The corresponding results are shown in Fig.6. This figure exhibits following features

(a) In the MSSM, a suppressed $Z\gamma$ signal (compared with its SM prediction) tend to correspond to an enhanced $b\bar{b}$ signal, and an enhanced $Z\gamma$ signal requires the $b\bar{b}$ signal rates to be roughly at its SM prediction. In any case, the enhancement factor for the

two signals are less than 1.2. Note there exit few cases where the $b\bar{b}$ signal rate is slightly suppressed.

(b) In the NMSSM with large λ, the normalized $b\bar{b}$ signal rate is less than 1.1, and in some cases, it may be significantly suppressed. In contrast, the $Z\gamma$ signal rate can be either greatly enhanced or severely suppressed. In the enhancement case, the $b\bar{b}$ signal rate is usually less than its SM prediction, and the greater enhancement corresponds to the stronger suppression.

(c) In the CMSSM, both the signal rates are roughly equal to their SM predictions, and in the nMSSM, both the rates are strongly suppressed.

Furthermore, we checked that the $\gamma\gamma$ signal rate at the ILC has similar dependence on the $b\bar{b}$ rate for the four models.

IV. CONCLUSION

In this work, we investigated the rare decay of the SM-like Higgs boson, $h \to Z\gamma$, and studied its correlations with $h \to \gamma\gamma$ in low energy SUSY models. We performed a scan over the parameter space of each model by considering various experimental constraints and presented our results only in the experimentally allowed parameter space. We have following observations:

(i) In SUSY models, the correction to the amplitude of $h \to Z\gamma$ induced by a certain sparticle is correlated with that of $h \to \gamma\gamma$, and the latter is usually several times larger in magnitude than the former.

(ii) In the MSSM, the net sparticle contribution to the amplitude of $h \to Z\gamma$ is constructive with the corresponding SM amplitude and can enhance the corresponding SM prediction by at most 10%. Consequently, the $Z\gamma$ signal rates at the LHC and the ILC can be enhanced by 20% at most. As a comparison, the $\gamma\gamma$ signal rates can be enhanced by a factor 2 due to large $\tilde{\tau}$ contributions.

(iii) In the CMSSM, due to the slightly enhanced $h \to b\bar{b}$ partial width, the $Z\gamma$ signal rates at the LHC and ILC are slightly below their SM predictions, which is quite similar to the behaviors of the $h \to \gamma\gamma$ channel.

(iv) In the NMSSM with large λ, the SUSY corrections to the amplitudes of $h \to Z\gamma$ and $h \to \gamma\gamma$ are at most 10%, and to get significant deviation of the two rates from their SM values, the $hb\bar{b}$ coupling must be moderately suppressed by the singlet component of h. In this model, the two rates are highly correlated and vary from 0.2 to 2.

(v) In the nMSSM, the signal rates of $h \to Z\gamma$ and $h \to \gamma\gamma$ are both greatly suppressed due to the possible exotic decay $h \to \chi^0\chi^0, AA$.

Since different SUSY models predict different correlation behaviors between the $Z\gamma$ and $\gamma\gamma$ rates, and some non-SUSY models also predict rather different correlation behaviors [6], such a correlation may play an important role in testing the Higgs property and distinguishing the relevant new physics models in future.

Acknowledgement

We thank Kun Yao and Jingya Zhu for helpful discussions. This work was supported in part by the National Natural Science Foundation of China (NNSFC) under grant No. 10775039, 11075045, 11275245, 10821504 and 11135003, by the Project of Knowledge Innovation Program (PKIP) of Chinese Academy of Sciences under grant No. KJCX2.YW.W10.

Appendix

In SUSY, the decays $h \to Z\gamma$ and $h \to \gamma\gamma$ get new contributions from the loops mediated by charged Higgs bosons, sfermions (including stops, sbottoms and staus) and charginos, and as a result, the formula of $\Gamma_{Z\gamma}$ and $\Gamma_{\gamma\gamma}$ are modified by

$$\Gamma(h \to Z\gamma) = \frac{G_F^2 m_W^2 \,\alpha\, m_h^3}{64\,\pi^4}\left(1-\frac{m_Z^2}{m_h^2}\right)^3 \left|\mathcal{A}_W^{Z\gamma}+\mathcal{A}_t^{Z\gamma}+\mathcal{A}_{H^\pm}^{Z\gamma}+\mathcal{A}_{\tilde{f}_i}^{Z\gamma}+\mathcal{A}_{\chi_i^\pm}^{Z\gamma}\right|^2 \quad (14)$$

$$\Gamma(h \to \gamma\gamma) = \frac{G_F \alpha^2 m_h^3}{128\sqrt{2}\pi^3}\left|\mathcal{A}_W^{\gamma\gamma}+\mathcal{A}_t^{\gamma\gamma}+\mathcal{A}_{H^\pm}^{\gamma\gamma}+\mathcal{A}_{\tilde{f}_i}^{\gamma\gamma}+\mathcal{A}_{\chi_i^\pm}^{\gamma\gamma}\right|^2. \quad (15)$$

The expressions of $A_i^{\gamma\gamma}$ are relatively simple and are given by

$$\mathcal{A}_W^{\gamma\gamma} = g_{hVV}A_1(\tau_W),\ \mathcal{A}_t^{\gamma\gamma} = g_{ht\bar{t}}N_c Q_t^2 A_{1/2}(\tau_t),\ \mathcal{A}_{\tilde{f}_i}^{\gamma\gamma} = \sum_i \frac{g_{h\tilde{f}_i\tilde{f}_i}}{m_{\tilde{f}_i}^2}N_c Q_{\tilde{f}_i}^2 A_0(\tau_{\tilde{f}_i}),$$

$$\mathcal{A}_{H^\pm}^{\gamma\gamma} = \frac{m_Z^2 g_{hH^+H^-}}{2M_{H^\pm}^2}A_0(\tau_{H^\pm}),\ \mathcal{A}_{\chi_i^\pm}^{\gamma\gamma} = \sum_i \frac{2m_W}{m_{\chi_i^\pm}}g_{h\chi_i^+\chi_i^-}A_{1/2}(\tau_{\chi_i^\pm}), \quad (16)$$

where $\tau_i = 4m_i^2/m_h^2$, g_{hXY} denotes the Higgs coupling with particles XY and $A_0, A_{1/2}$ and A_1 are loop functions with scalars, fermions and gauge bosons running in the loop. The explicit expressions of g_{hXY} and A functions are given by

$$g_{hVV} = S_{h1}\sin\beta + S_{h2}\cos\beta, \tag{17}$$

$$g_{ht\bar{t}} = S_{h1}/\sin\beta, \tag{18}$$

$$g_{h\tilde{f}_1\tilde{f}_1} = \frac{-1}{2(\sqrt{2}G_F)^{1/2}}\left(\mathrm{Y}_{hLL}\cos^2\theta_{\tilde{f}} + \mathrm{Y}_{hRR}\sin^2\theta_{\tilde{f}} + \mathrm{Y}_{hLR}\sin 2\theta_{\tilde{f}}\right), \tag{19}$$

$$g_{h\tilde{f}_2\tilde{f}_2} = \frac{-1}{2(\sqrt{2}G_F)^{1/2}}\left(\mathrm{Y}_{hLL}\sin^2\theta_{\tilde{f}} + \mathrm{Y}_{hRR}\cos^2\theta_{\tilde{f}} - \mathrm{Y}_{hLR}\sin 2\theta_{\tilde{f}}\right), \tag{20}$$

$$\begin{aligned} g_{hH^+H^-} = {} & \frac{\lambda^2}{\sqrt{2}}\left(v_s(\Pi^{11}_{h3}+\Pi^{22}_{h3}) - v_u\Pi^{12}_{h2} - v_d\Pi^{12}_{h1}\right) + \sqrt{2}\lambda\kappa v_s\Pi^{12}_{h3} + \frac{\lambda}{\sqrt{2}}A_\lambda\Pi^{12}_{h3} \\ & + \frac{g_1^2}{4\sqrt{2}}\left(v_u(\Pi^{11}_{h1}-\Pi^{22}_{h1}) + v_d(\Pi^{22}_{h2}-\Pi^{11}_{h2})\right) \\ & + \frac{g_2^2}{4\sqrt{2}}\left(v_u(\Pi^{11}_{h1}+\Pi^{22}_{h1}+2\Pi^{12}_{h2}) + v_d(\Pi^{11}_{h2}+\Pi^{22}_{h2}+2\Pi^{12}_{h1})\right), \end{aligned}$$

$$\Pi^{jk}_{hi} = 2S_{hi}C_jC_k, \quad C_1 = \cos\beta, \quad C_2 = \sin\beta,$$

$$v_u = \frac{1}{(\sqrt{2}G_F)^{1/2}}C_2, \quad v_d = \frac{1}{(\sqrt{2}G_F)^{1/2}}C_1, \quad v_s = \mu/\lambda, \tag{21}$$

$$g^L_{h\chi_i^+\chi_j^-} = \frac{1}{\sqrt{2}}(S_{h1}U_{i1}V_{j2} + S_{h2}U_{i2}V_{j1}), \quad g^R_{h\chi_i^+\chi_j^-} = \frac{1}{\sqrt{2}}(S_{h1}U_{j1}V_{i2} + S_{h2}U_{j2}V_{i1}), \tag{22}$$

$$A_0(x) = -x^2\left[x^{-1} - f(x^{-1})\right], \tag{23}$$

$$A_{1/2}(x) = 2\,x^2\left[x^{-1} + (x^{-1}-1)f(x^{-1})\right], \tag{24}$$

$$A_1(x) = -x^2\left[2x^{-2} + 3x^{-1} + 3(2x^{-1}-1)f(x^{-1})\right], \tag{25}$$

where S is the 2×2 (3×3) rotation matrix of MSSM (NMSSM) higgs mass matrix under the basis (H_u^0, H_d^0, S), h in S_{h1} denotes the row index of the SM-like Higgs, Y_{hXY} denotes the SM-like higgs coupling to sfermion interaction states, U, V denote the rotation matrices of the chargino mass matrix, and $f(x)$ is defined by $f(x) = \arcsin^2\sqrt{x}$.

As for $A_i^{Z\gamma}$, due to $m_Z \neq 0$ and the existence of ZXY ($X \neq Y$) couplings, their expres-

sions are rather complex

$$
\begin{aligned}
&\mathcal{A}_W^{Z\gamma} = g_{hVV} c_w A_1(\tau_W, \lambda_W),\ \mathcal{A}_t^{Z\gamma} = g_{ht\bar{t}} N_c\, Q_t \frac{\hat{v}_t}{c_w}\, A_{1/2}(\tau_t, \lambda_t),\\
&\mathcal{A}_{H^\pm}^{Z\gamma} = -\frac{m_Z^2 g_{hH^+H^-}}{2\, m_{H^\pm}^2} v_{H^\pm} A_0(\tau_{H^\pm}, \lambda_{H^\pm}),\\
&\mathcal{A}_{\tilde{f}_i}^{Z\gamma} = -\sum_{\tilde{f}_i} \frac{2\, g_{h\tilde{f}_i\tilde{f}_i}}{m_{\tilde{f}_i}^2} N_c Q_{\tilde{f}_i} v_{\tilde{f}_i} A_0(\tau_{\tilde{f}_i}, \lambda_{\tilde{f}_i}) - \mathcal{A}_{\tilde{f}_1\tilde{f}_2}^{Z\gamma},\\
&\mathcal{A}_{\tilde{f}_1\tilde{f}_2}^{Z\gamma} = \frac{2\, g_{h\tilde{f}_1\tilde{f}_2}}{m_{\tilde{f}_1} m_{\tilde{f}_2}} N_c Q_{\tilde{f}} v_{\tilde{f}_{12}} (A_0^{(1)} + A_0^{(2)}),\\
&\mathcal{A}_{\chi_i^\pm}^{Z\gamma} = \sum_{\chi_i^\pm; m,n=L,R} \frac{2m_W}{m_{\chi_i^\pm}} g^m_{h\chi_i^+\chi_i^-} g^n_{Z\chi_i^+\chi_i^-} A_{1/2}(\tau_{\chi_i^\pm}, \lambda_{\chi_i^\pm}) + \mathcal{A}_{\chi_1^+\chi_2^-}^{Z\gamma},\\
&\mathcal{A}_{\chi_1^+\chi_2^-}^{Z\gamma} = \frac{2m_W}{\sqrt{m_{\chi_1^\pm} m_{\chi_2^\pm}}} \Big((g^L_{h\chi_1^+\chi_2^-} g^L_{Z\chi_1^+\chi_2^-} + g^R_{h\chi_1^+\chi_2^-} g^R_{Z\chi_1^+\chi_2^-}) A_{1/2}^{(1)},\\
&\qquad\qquad + (g^L_{h\chi_1^+\chi_2^-} g^R_{Z\chi_1^+\chi_2^-} + g^R_{h\chi_1^+\chi_2^-} g^L_{Z\chi_1^+\chi_2^-}) A_{1/2}^{(2)} \Big),
\end{aligned}
\tag{26}
$$

where $\lambda_i = 4m_i^2/m_Z^2$ and the coupling coefficients of h and Z are given by

$$\hat{v}_t = 2T_3^t - 4Q_t s_w^2, \quad v_{H^\pm} = (c_w^2 - s_w^2)/c_w, \tag{27}$$

$$v_{\tilde{f}_1} = (T_f^3 \cos^2\theta_{\tilde{f}} - Q_f s_w^2)/c_w, \qquad v_{\tilde{f}_2} = (T_f^3 \sin^2\theta_{\tilde{f}} - Q_f s_w^2)/c_w, \tag{28}$$

$$v_{\tilde{f}_{12}} = (-T_f^3 \sin\theta_{\tilde{f}} \cos\theta_{\tilde{f}})/c_w, \tag{29}$$

$$g_{h\tilde{f}_1\tilde{f}_2} = \frac{-1}{2(\sqrt{2}G_F)^{1/2}} \left(\frac{1}{2} (\mathrm{Y}_{hRR} - \mathrm{Y}_{hLL}) \sin 2\theta_{\tilde{f}} + \mathrm{Y}_{hLR} \cos 2\theta_{\tilde{f}} \right), \tag{30}$$

$$g^L_{Z\chi_1^+\chi_1^-} = (V_{11}^2 + 1 - 2s_w^2)/(2\, c_w), \qquad g^R_{Z\chi_1^+\chi_1^-} = (U_{11}^2 + 1 - 2s_w^2)/(2\, c_w), \tag{31}$$

$$g^L_{Z\chi_2^+\chi_2^-} = (V_{21}^2 + 1 - 2s_w^2)/(2\, c_w), \qquad g^R_{Z\chi_2^+\chi_2^-} = (U_{21}^2 + 1 - 2s_w^2)/(2\, c_w), \tag{32}$$

$$g^L_{Z\chi_1^+\chi_2^-} = (V_{11} V_{21})/(2\, c_w), \qquad g^R_{Z\chi_1^+\chi_2^-} = (U_{11} U_{21})/(2\, c_w). \tag{33}$$

In above formula, we have defined some new functions as

$$
\begin{aligned}
&A_0^{(1)} = 4 m_{\tilde{f}_1} m_{\tilde{f}_2} (C_{23}^{(1)} + C_{12}^{(1)})\\
&A_0^{(2)} = 4 m_{\tilde{f}_1} m_{\tilde{f}_2} (C_{23}^{(2)} + C_{12}^{(2)})\\
&A_{1/2}^{(1)} = 2 m_{\chi_1^\pm} \sqrt{m_{\chi_1^\pm} m_{\chi_2^\pm}} \left((2C_{23}^{(3)} + 3C_{12}^{(3)} + C_0^{(3)}) + (2C_{23}^{(4)} + C_{12}^{(4)}) \right)\\
&A_{1/2}^{(2)} = 2 m_{\chi_2^\pm} \sqrt{m_{\chi_1^\pm} m_{\chi_2^\pm}} \left((2C_{23}^{(4)} + 3C_{12}^{(4)} + C_0^{(4)}) + (2C_{23}^{(3)} + C_{12}^{(3)}) \right)
\end{aligned}
\tag{34}
$$

with C_{ij} denoting three points loop functions introduced in [33], and $C^{(1)} = C(P_\gamma, P_Z, m_{\tilde{f}_1}, m_{\tilde{f}_1}, m_{\tilde{f}_2})$, $C^{(2)} = C^{(1)}|_{m_{\tilde{f}_1} \leftrightarrow m_{\tilde{f}_2}}$, $C^{(3)} = C^{(1)}|_{m_{\tilde{f}_1} \to m_{\chi_1^\pm}, m_{\tilde{f}_2} \to m_{\chi_2^\pm}}$, and $C^{(4)} =$

$C^{(3)}|_{m_{\chi_1^\pm} \leftrightarrow m_{\chi_2^\pm}}$. For the special cases considered here, C_{ij} are given by

$$C_0(p_\gamma, p_Z, m_1, m_1, m_2) = -\int_0^1 dy \frac{1}{b} \ln|\frac{by+c}{c}| \tag{35}$$

$$C_{12}(p_\gamma, p_Z, m_1, m_1, m_2) = \int_0^1 dy \frac{1-y}{b} \ln|\frac{by+c}{c}| \tag{36}$$

$$C_{23}(p_\gamma, p_Z, m_1, m_1, m_2) = \int_0^1 dy \frac{y(1-y)}{b}\left(1 - \frac{b+c}{by} \ln|\frac{by+c}{c}|\right) \tag{37}$$

where

$$b = -(m_h^2 - m_Z^2)(1-y), \quad c = -m_Z^2 y(1-y) + m_1^2 y + m_2^2(1-y). \tag{38}$$

Note that for the special case $m_1 = m_2$, these functions can be further simplified to get their analytic expressions. The other functions relevant to our calculation are defined by

$$A_0(x,y) = I_1(x,y), \tag{39}$$

$$A_{1/2}(x,y) = I_1(x,y) - I_2(x,y), \tag{40}$$

$$A_1(x,y) = 4(3 - \tan^2\theta_w) I_2(x,y) + \left[(1+2x^{-1})\tan^2\theta_w - (5+2x^{-1})\right] I_1(x,y), \tag{41}$$

with

$$I_1(x,y) = \frac{xy}{2(x-y)} + \frac{x^2y^2}{2(x-y)^2}[f(x^{-1}) - f(y^{-1})] + \frac{x^2 y}{(x-y)^2}[g(x^{-1}) - g(y^{-1})], \tag{42}$$

$$I_2(x,y) = -\frac{xy}{2(x-y)}[f(x^{-1}) - f(y^{-1})], \tag{43}$$

$$g(x) = \sqrt{x^{-1} - 1}\arcsin\sqrt{x}. \tag{44}$$

---

[1] G. Aad et al. [ATLAS Collaboration], Phys. Lett. B 716, 1 (2012); S. Chatrchyan et al. [CMS Collaboration], Phys. Lett. B 716, 30 (2012).

[2] G. Aad et al. [ATLAS Collaboration], ATLAS-CONF-2012-162; S. Chatrchyan et al. [CMS Collaboration], CMS-PAS-HIG-12-042; CMS-PAS-HIG-12-044; CMS-PAS-HIG-12-043.

[3] Y. Gao et al., Phys. Rev. D 81, 075022 (2010); J. Ellis and D. S. Hwang, JHEP **1209**, 071 (2012).

[4] M. Carena, I. Low and C. E. M. Wagner, JHEP **1208**, 060 (2012).

[5] A. G.Akeroyd and S. Moretti, Phys. Rev. D 86, 035015 (2012); A. Kobakhidze, arXiv:1208.5180; L. Wang and X. -F. Han, arXiv:1209.0376; M. Carena *et al.*, arXiv:1211.6136; E. J. Chun *et al.*, JHEP 1211, 106 (2012); R. Sato *et al.*,Phys. Lett. B 716, 441 (2012); W. -C. Huang and A. Urbano, arXiv:1212.1399; M. Chala, arXiv:1210.6208; E. O. Iltan, arXiv:1212.5695.

[6] C. Han *et al.*, arXiv:1212.6728 [hep-ph]; I. Picek and B. Radovcic, arXiv:1210.6449.

[7] A. Joglekar *et al.*, arXiv:1207.4235; E. Bertuzzo *et al.*, arXiv:1209.6359; L. G. Almeida *et al.*, JHEP 1211, 085 (2012); H. Davoudiasl *et al.*,arXiv:1211.3449; B. Batell *et al.*, arXiv:1211.2449; H. M. Lee *et al.*, arXiv:1209.1955; M. B. Voloshin, Phys. Rev. D 86, 093016 (2012); N. Bonne and G. Moreau, Phys. Lett. B717, 409 (2012); S. Dawson and E. Furlan,Phys. Rev. D86, 015021 (2012); M. A. Ajaib, I. Gogoladze, Q. Shafi, arXiv:1207.7068; S. Dawson *et al.*, arXiv:1210.6663.

[8] A. Alves *et al.*, Phys. Rev. D84, 115004 (2011); T. Abe, N. Chen and H. -J. He, arXiv:1207.4103.

[9] A. Urbano, arXiv:1208.5782.

[10] M. Carena *et al.* JHEP 1203, 014 (2012); JHEP **1207**, 175 (2012); U. Ellwanger, JHEP 1203, 044 (2012); U. Ellwanger, C. Hugonie, arXiv:1203.5048; A. Arbey *et al.*, JHEP **1209**, 107 (2012); K. Hagiwara, J. S. Lee, J. Nakamura, JHEP 1210, 002 (2012); R. Benbrik *et al.*, arXiv:1207.1096; T. Cheng, arXiv:1207.6392; B. Kyae, J.-C. Park, arXiv:1207.3126; H. An, T. Liu, L.-T. Wang, arXiv:1207.2473; J. Ke *et al.*, arXiv:1207.0990; G. Belanger *et al.*, arXiv:1208.4952; N. Liu *et al.*, arXiv:1208.3413; M. Drees, arXiv:1210.6507; S. F. King *et al.*, arXiv:1211.5074; K. Choi *et al.*, arXiv:1211.0875; M. Berg *et al.*, arXiv:1212.5009; L. Aparicio *et al.*, arXiv:1212.4808; C. Balazs, S. K. Gupta, arXiv:1212.1708; K. Cheung, C.-T. Lu, T.-C. Yuan, arXiv:1212.1288; Z. Kang, Y. Liu and G. Ning,arXiv:1301.2204; E. J. Chun and P. Sharma, arXiv:1301.1437.

[11] J. Cao *et al.*, Phys. Lett. B **710**, 665 (2012); Phys. Lett. B **703**, 462 (2011).

[12] J. Cao *et al.*, JHEP **1203**, 086 (2012); JHEP **1210**, 079 (2012).

[13] A. Drozd *et al.*, arXiv:1211.3580; G. Belanger*et al.*, arXiv:1212.5244; arXiv:1208.4952; P. M. Ferreira*et al.*, arXiv:1211.3131; S. Chang *et al.*, arXiv:1210.3439; S. Bar-Shalom *et al.*, arXiv:1208.3195; H. S. Cheon and S. K. Kang, arXiv:1207.1083; A. Arhrib *et al.*, arXiv:1205.5536; C. Chiang and K. Yagyu, arXiv:1207.1065; J. Chang *et al.*, arXiv:1206.5853;

L. Wang and X. -F. Han, Phys. Rev. D **87**, 015015 (2013); arXiv:1209.0376; N. Chen and H. -J. He, JHEP **1204**, 062 (2012); B. Swiezewska and M. Krawczyk, arXiv:1212.4100.

[14] K. Hsieh and C.-P. Yuan, Phys. Rev. D78, 053006 (2008); L. Wang and J. M. Yang, Phys. Rev. D84, 075024 (2011); J. Reuter and M. Tonini, arXiv:1212.5930; X. -F. Han, *et al.*, arXiv:1301.0090.

[15] J. S. Gainer *et al.*, Phys. Rev. D **86**, 033010 (2012); S. Choi, M. Muhlleitner and P. Zerwas, arXiv:1209.5268.

[16] C. Chiang and K. Yagyu, arXiv:1207.1065; P. Castaneda-Almanza and A. Gutierrez-Rodriguez, Electron. J. Theor. Phys. PS **8**, 133 (2011); P. S. B. Dev *et al.*, arXiv:1301.3453.

[17] B. Coleppa, K. Kumar, H. E. Logan, arXiv:1208.2692; I. Dorsner, S. Fajfer, A. Greljo and J. F. Kamenik, JHEP **1211**, 130 (2012) [arXiv:1208.1266 [hep-ph]]; G. Chalons and F. Domingo, Phys. Rev. D **86**, 115024 (2012) [arXiv:1209.6235 [hep-ph]].

[18] CMS Collaboration, HIG-12-049-pas; ATLAS Collaboration, ATLAS-CONF-2013-009.

[19] J. E. Kim and H. P. Nilles, Phys. Lett. B **138**, 150 (1984).

[20] A. Djouadi *et al.* [MSSM Working Group Collaboration], hep-ph/9901246.

[21] C. -S. Chen, C. -Q. Geng, D. Huang and L. -H. Tsai, arXiv:1301.4694 [hep-ph].

[22] A.H. Chamseddine, R. Arnowitt and P. Nath, Phys. Rev. Lett. 49 (1982) 970; R. Barbieri, S. Ferrara and C.A Savoy, Phys. Lett. B119 (1982) 343; L. Hall, J. Lykken and S. Weinberg, Phys. Rev. D27 (1983) 2359; N. Ohta, "Grand Unified Theories Based on Local Supersymmetry," Prog. Theor. Phys. 70 (1983) 542;

[23] U. Ellwanger, C. Hugonie and A. M. Teixeira, Phys. Rept. 496, 1 (2010); M. Maniatis, Int. J. Mod. Phys. A25 (2010) 3505; J. R. Ellis *et al.* Phys. Rev. D **39**, 844 (1989); M. Drees, Int. J. Mod. Phys. A**4**, 3635 (1989); S. F. King, P. L. White, Phys. Rev. D **52**, 4183 (1995); B. Ananthanarayan, P.N. Pandita, Phys. Lett. B **353**, 70 (1995); B. A. Dobrescu, K. T. Matchev, JHEP **0009**, 031 (2000); R. Dermisek, J. F. Gunion, Phys. Rev. Lett. **95**, 041801 (2005); G. Hiller, Phys. Rev. D **70**, 034018 (2004); F. Domingo, U. Ellwanger, JHEP **0712**, 090 (2007); Z. Heng *et al.*, Phys. Rev. D **77**, 095012 (2008); R. N. Hodgkinson, A. Pilaftsis, Phys. Rev. D **76**, 015007 (2007); W. Wang *et al.* Phys. Lett. B **680**, 167 (2009); J. M. Yang, arXiv:1102.4942; U. Ellwanger and C. Hugonie, arXiv:hep-ph/0612133; arXiv:hep-ph/9909260; U. Ellwanger, arXiv:1108.0157.

[24] P. Fayet, Nucl. Phys. B 90, 104 (1975); A. Menon, et al., Phys. Rev. D 70, 035005 (2004);

V. Barger, et al., Phys. Lett. B 630, 85 (2005); C. Balazs, et. al., JHEP 0706, 066 (2007); C. Panagiotakopoulos, K. Tamvakis, Phys. Lett. B 446, 224 (1999); Phys. Lett. B 469, 145 (1999); C. Panagiotakopoulos, A. Pilaftsis Phys. Rev. D 63, 055003 (2001); A. Dedes, et. al., Phys. Rev. D 63, 055009 (2001); J. Cao, H. E. Logan and J. M. Yang, Phys. Rev. D **79**, 091701 (2009); K. S. Jeong, Y. Shoji and M. Yamaguchi, JHEP **1204**, 022 (2012); JHEP **1209**, 007 (2012).

[25] J. Cao, H. E. Logan and J. M. Yang, Phys. Rev. D **79**, 091701 (2009).

[26] J.Cao *et al.*, JHEP **1206**, 145 (2012).

[27] A. Djouadi, Phys. Rept. **459**, 1 (2008).

[28] U. Ellwanger, J. F. Gunion and C. Hugonie, JHEP 0502, 066 (2005); U. Ellwanger and C. Hugonie, Comput. Phys. Commun. 175, 290 (2006); G. Degrassi et al., Eur. Phys. J. C 28 (2003) 133.

[29] S. Heinemeyer, W. Hollik and G. Weiglein, Eur. Phys. J. C 9 (1999) 343; S. Heinemeyer, W. Hollik and G. Weiglein, Comput. Phys. Commun. 124 (2000) 76; M. Frank et al., JHEP 0702 (2007) 047.

[30] Dark Attack 2012 Conference Data, http://dmtools.brown.edu/

[31] The LHCb collaboration, arXiv:1211.2674;

[32] The CMS Collaboration, HIG-12-051-pas.

[33] A. Axelrod, Nucl. Phys. B 209, 349 (1982).